

Pore-Level Study of the Effect of Miscibility and Wettability on Oil Recovery during Gas Assisted Gravity Drainage

H. Khorshidian, L.A. James, and S.D. Butt

Memorial University of Newfoundland

This paper was prepared for presentation at the International Symposium of the Society of Core Analysts held in Vienna, Austria, 27 August - 1 September 2017

ABSTRACT

The effect of the gas-oil interfacial tension and wettability on the performance of gas assisted gravity drainage (GAGD) process was investigated at the pore-level to explore conditions leading to high oil recoveries. This work extends the previous investigation of GAGD parameters, i.e., the contribution of film flow and wettability, that we presented in 2015 and 2016. GAGD experiments were conducted in a new micromodel with an improved capillary continuity to reflect mechanisms of oil recovery effectively. The result of the experiment showed that the heterogeneities of the porous medium causes the gas-front to bypass oil in small pores surrounded by large pores. The subsequent drainage of bypassed pores was possible where the gas-oil capillary pressure was sufficiently increased due to a reduction in the hydrostatic pressure of oil. The strong hydraulic continuity of oil in an oil-wet porous medium compared to a water-wet porous medium contributed to a low residual oil saturation under immiscible conditions. In water-wet micromodels, a near-complete oil recovery was obtained under miscible conditions as no interface between oil and gas was formed, and no oil was bypassed when the miscible displacement is developed.

INTRODUCTION

Gas Assisted Gravity Drainage (GAGD) is an effective method of oil recovery influenced by the reservoir rock and fluids' properties, such as the state of wettability [1, 2], heterogeneities [3, 4], and interfacial tension between the fluids [5, 6]. During GAGD, the entry of gas into an oil-occupied pore occurs when the gas-oil capillary pressure is sufficiently increased. [7]. The capillary pressure between two phases is directly proportional to their interfacial tension and inversely proportional to the pore size. Therefore, the gas-oil capillary pressure in larger pores is lower so drainage of oil initially begins from larger pores [8]. The gas-front may bypass smaller oil-occupied pores that are surrounded by larger pores [4]. In gas-invaded zones, thick films of oil may be retained in fine capillaries of a porous medium formed around the rock grains and on their rough surfaces. In the gravity drainage, these fine capillaries provide the wetting phase with continuous paths to maintain strong hydraulic continuity linking the bypassed pores to pores at lower elevations [9]. Under such conditions, the hydrostatic pressure of oil in bypassed pores decreases at higher elevations from the gas-front. Therefore, the local gas-oil capillary pressure in a bypassed pore at greater elevations can be higher than the gas-oil capillary pressure in the gas-front when a hydraulic communication between the bypassed pore and gas-front is maintained [10]. The fine capillaries of a porous medium,

depending on their length and geometry, contribute to a limited increase of the gas-oil capillary pressure beyond which the hydraulic continuity of oil is terminated [10, 11].

The reduction of the gas-oil interfacial tension decreases the gas-oil capillary pressure at the gas-oil interface. Therefore, a better GAGD performance might be expected with a reduction in capillary forces allowing gravitational forces to drain the liquid more easily. However, the injection of a rich gas may also reduce the gas-oil differential density dissolving in oil.

In GAGD, the stability of the gas-front, in addition to heterogeneities of the porous medium, is controlled by the gas-oil interfacial tension. The gas-front normally bypasses oil when gas-oil interfaces in larger pores (leading zones) surround gas-oil interfaces in smaller pores (trailing zones). Fig. 1 schematically shows drainage of oil by gas in a porous medium containing large and small pores. When the viscous forces are negligible, the minimum vertical distance (D_{\min}) between the leading and trailing gas-oil interfaces prior to the bypass of oil can be calculated by Eq. 1,

$$D_{\min} = \frac{P_{\text{cgo}}^{\text{T}} - P_{\text{cgo}}^{\text{L}}}{\Delta\rho_{\text{go}}g} \quad (1)$$

where $P_{\text{cgo}}^{\text{T}}$ and $P_{\text{cgo}}^{\text{L}}$ are the gas-oil capillary pressure in the trailing and leading zones respectively, and $\Delta\rho_{\text{go}}$ is the gas-oil differential density. In a system with a fixed pore size distribution, decreasing the gas-oil interfacial tension lowers variations of gas-oil capillary pressure in various pore sizes (numerator in Eq. 1). Therefore, a reduction of the gas-oil interfacial tension and an increase of the gas-oil differential density can stabilize the gas-front and eventually reduce the size of a bypassed zone (Fig. 1c).

A further reduction of the gas-oil interfacial tension may lead to miscible oil displacement conditions depending on oil and gas composition, temperature and injection pressure [12]. Under miscible conditions, in addition to a direct oil displacement, the extraction of oil by gas and swelling of oil volume are the main mechanisms of the oil recovery [13, 14].

In our previous work, the effect of wettability on the GAGD performance was studied in a micromodel with poor capillary continuity. In this work, a new micromodel with improved capillary continuity has been developed to investigate the effect the gas-oil interfacial tension on the GAGD performance under oil-wet and water-wet conditions to identify the effect of wettability on residual oil saturations varying the gas-oil interfacial tensions.

EXPERIMENTAL DETAILS

A new pore network micromodel with an improved capillary continuity was fabricated bonding two acrylic (Plexiglas®) plates containing coarse pores and fine capillaries. The coarse pore network (Fig. 2) is made by repeating a designed pattern (Fig. 3) containing pore sizes in the range of 150 - 1300 μm . The designed pore network was etched by CO_2 laser on an acrylic plate, and the depth of etching was in the range of 140 - 160 μm . Another plate of the micromodel was scratched with a grit 60 sandpaper to form fine capillaries covering the coarse pore network from the top port to the bottom port. The porosity of the designed pattern is 0.48, and the pore volume (PV) of the micromodel is 0.940 ± 0.005 ml. The pore sizes of the micromodel are one order of magnitude larger than the pore sizes in

a sandstone. The magnification of the pore structure reduces the capillary forces compared to the gravitational forces. This helps us to study the interaction of capillary and gravitational forces in a system with limited height. In addition, fluid saturations are quantified via image analysis and error due to resolution is less relative to larger pores. The fluid saturations in the micromodel were calculated using an in-house developed image analysis methodology that evaluates the colour of pixels (red: oil and blue: water) in the recorded pictures during an experiment. The fluid saturation and recovery factor can be calculated with respect to the total number of pixels (with red, blue and white colours) and micromodel porosity. The associated uncertainty with the calculated saturations is $\pm 2\%$.

The wettability of the micromodel was varied from a strongly oil-wet condition to a strongly water-wet condition as described in the previous work [10]. Fig. 3a and Fig. 3c show images of the repeated pattern in the oil-wet and water-wet micromodels, respectively (note films of the wetting phase in narrow fine capillaries).

GAGD tests were conducted at 24°C injecting CO_2 and C_3H_8 (99% purity) under fixed pressure (4.0 bars in immiscible tests and 8.4 bars in a miscible test) from the top port of the micromodel. A precision piston pump (Quizix 20K series) was used to produce fluids from the bottom port of the micromodel at a constant rate (0.1 ml/hr in immiscible tests and 0.3 ml/hr in a miscible test). The initial oil and water saturations under the oil-wet condition is established by injecting 5 PV water (blue dyed) into a fully oil-occupied micromodel at a flow rate of 5 ml/min followed by injecting 10 PV of oil (red dyed Varsol™ without dissolved gas) at a flow rate of 5 ml/min to establish a low water saturation. Under water-wet conditions, the fully water-occupied micromodel is flooded by 10 PV of oil at a flow rate of 5 ml/min.

Table 1 shows the interfacial tension between test fluids at the corresponding conditions measured with VINCI IFT 700 apparatus. Table 2 also shows the composition of oil (Varsol™) measured with Agilent 7890 distillation system. In addition, equilibrium swelling of oil volume when contacted by C_3H_8 and CO_2 was measured at test conditions (4.0 bars and 24°C). The volume of oil in equilibrium with C_3H_8 was increased by $32 \pm 1\%$, but no significant swelling of oil was observed with CO_2 . The density of live oil containing C_3H_8 at equilibrium was measured at 0.705 ± 0.001 g/ml using Anton Paar DMA-HPM density apparatus.

RESULTS & DISCUSSION

The GAGD experimental results are presented in Table 3 showing the variation of fluids' saturation and ultimate oil recoveries. Fig. 4 and Fig. 5 show the micromodel images during GAGD tests performed with CO_2 in the oil-wet and water-wet micromodels, respectively. In both wettability conditions, the bypass of oil with the gas-front occurred in pores where a higher gas-oil capillary pressure must be overcome compared to their neighboring pores (e.g. smaller pores surrounded by larger pores). The average residual oil saturation in GAGD tests performed using CO_2 at the time of the gas-breakthrough was $0.31 \text{ PV} \pm 1.4\%$ in the oil-wet micromodel, and $0.35 \text{ PV} \pm 1.4\%$ in the water-wet micromodel. The average residual oil saturation after 2 PV production (total test duration: 19 hrs) was $0.21 \text{ PV} \pm 1.4\%$ and $0.31 \text{ PV} \pm 1.4\%$ in oil-wet and water-wet conditions, respectively. Similar results were obtained when experiments were repeated but with varied bypassed residual oil zones.

The difference in the initial positioning of the water saturation was the major source of variation in results of repeated experiments.

In the oil-wet micromodel, additional recovery from initially bypassed pores was obtained after the gas-breakthrough via film flow mechanism [10]. The fine capillaries maintained the hydraulic continuity of oil between zones at different elevations and provided a continuous path for the flow of oil. Therefore, a low residual oil saturation was obtained due to an effective increase of the gas-oil capillary pressure at higher elevations. Fig. 6a shows the ultimate state of the residual oil saturation in the oil-wet micromodel. In addition to small pores and around the solid grains, the residual oil was also found in the pores with entries blocked by water. Under such conditions (Fig. 6a), the cumulative capillary pressure required to simultaneously displace the gas-water and water-oil interfaces is high, and may lead to the retention of oil depending the size of the pore and geometry of local fine capillaries.

Fig. 6b shows the ultimate residual oil in the water-wet micromodel that is retained in larger pores than in the oil-wet micromodel. Under water-wet conditions, paths of the oil drainage in certain regions was blocked by the presence of water in smaller pores. In addition, the presence of water around the solid grains and corners of the fine capillaries restricted the hydraulic continuity of oil for an effective increase of the gas-oil capillary pressure. Consequently, the flow of oil in the form of thick films in water-wet media is restricted and resulted in a slight reduction of the residual oil saturation (0.04 PV) after approximately 15 hrs of production post gas-breakthrough.

The central region of the pore network contains wide channels forming a larger scale of heterogeneity, i.e., fracture. During GAGD, the leading edge of the gas-front was formed in wide channels causing the bypass of oil in the matrices. Under oil-wet conditions, the bypassed oil was subsequently recovered from the matrix because of the strong hydraulic continuity of oil. However, in the water-wet micromodel, the subsequent drainage of the bypassed oil from matrices was low due to weak hydraulic continuity oil.

The immiscible GAGD experiments were also performed with C_3H_8 (pressure: 4.0 bar, production rate: 0.1 ml/hr) to study the influence of a reduced gas-oil interfacial tension on GAGD performance. Figs. 7a & 7b. show the oil-wet and water-wet micromodels after 2 PV production, respectively. The ultimate residual oil saturation under oil-wet conditions was similar for both gas types. Under the water-wet condition, the variation of the gas type resulted in a slight reduction (0.03 PV) of the residual oil saturation.

In the oil-wet micromodel, because of strong hydraulic continuity of oil, the oil saturation in bypassed zones was effectively reduced when the vertical distance between these zones and the outlet port is sufficiently increased. Ultimately, the residual oil was retained in regions where hydraulic continuity of oil was terminated due to the geometric constraints of fine capillaries. In the water-wet micromodel, reducing the size of bypassed zones, with the reduction of the gas-oil interfacial tension to gas-oil differential density ratio, could decrease of the ultimate residual oil saturation particularly in zones where the hydraulic continuity of oil to lower elevations was not maintained. The injection of C_3H_8 instead of CO_2 improved the ultimate oil recovery factor due to swelling of the residual oil volume. However, this mechanism may become ineffective in a reservoir containing live oil.

An additional GAGD test was performed in a water-wet micromodel by injecting C_3H_8 at 8.4 bars to develop a miscible oil displacement (Fig. 8). The miscible gas injection, stabilized by gravity, resulted in an oil recovery factor of more than 99%. The small volume of the unrecovered oil was found in zones surrounded by water. In a miscible displacement, a region of swelled oil containing a high concentration of dissolved gas was developed between the gas and oil. A fully-developed transition zone formed with no interface with gas on top and oil on bottom. Consequently, a high recovery of oil was obtained by eliminating capillarity. The miscible oil displacement was gravity stable with the lowest density of gas being on top and increasing in the direction of gravity.

The GAGD experimental results in micromodels with improved capillary continuity showed that high oil recovery is obtained under oil-wet conditions. Under water-wet conditions, the positive influence of the gravitational force on the immiscible displacement of oil is limited by the presence of water. Miscible gas-oil displacement is very effective in obtaining very high recovery under all conditions including water-wet conditions.

CONCLUSIONS

During immiscible GAGD processes, heterogeneities of porous media caused the gas-front to bypass oil in smaller pores surrounded by larger pores. Under oil-wet conditions, the strong hydraulic communication of oil contributed to an additional oil recovery from initially bypassed regions where the gas-oil capillary pressure was effectively increased. However, under water-wet conditions, the presence of residual water in smaller pores and around the solid grains restricted the flow of oil from bypassed zones, and residual oil was retained at higher saturations. A reduction in the ratio of the gas-oil interfacial tension and gas-oil differential density slightly improved the GAGD performance in the water-wet micromodel. Very high oil recovery can be obtained with the displacement of oil under miscible conditions eliminating the capillarity at gas-oil interfaces in a heterogeneous porous medium.

Future Works

The cumulative oil-water capillary pressure that must be overcome for the simultaneous displacements of oil-water interfaces can be lowered in porous media with intermediate wetting conditions. In future works, the performance GAGD in slightly oil-wet and water-wet conditions will be evaluated and compared with the presented results.

ACKNOWLEDGEMENTS

The authors would like to thank Petroleum Research Newfoundland and Labrador (PRNL), Chevron Canada, Hibernia Management and Development Company (HMDC), Research and Development Corporation of Newfoundland and Labrador (RDC), the Natural Sciences and Engineering Research Council of Canada (NSERC) for financial support.

REFERENCES

1. Vizika, O. and J. Lombard, *Wettability and spreading: two key parameters in oil recovery with three-phase gravity drainage*. SPE Reservoir Engineering, 1996. **11**(01): p. 54-60.
2. Caubit, C., H. Bertin, and G. Hamon. Three-phase flow in porous media: wettability effect on residual saturations during gravity drainage and tertiary waterflood.

- presented in part at SPE Annual Technical Conference and Exhibition held in Houston Texas, USA, September 2004.
3. Parsaei, R. and I. Chatzis, *Experimental investigation of production characteristics of the gravity-assisted inert gas injection (GAIGI) process for recovery of waterflood residual oil: effects of wettability heterogeneity*. Energy & Fuels, 2011. **25**(5): p. 2089-2099.
 4. Catalan, L.J., F.A. Dullien, and I. Chatzis, *The effects of wettability and heterogeneities on the recovery of waterflood residual oil with low pressure inert gas injection assisted by gravity drainage*. SPE Advanced Technology Series, 1994. **2**(02): p. 140-149.
 5. Blunt, M., D. Zhou, and D. Fenwick, *Three-phase flow and gravity drainage in porous media*. Transport in porous media, 1995. **20**(1-2): p. 77-103.
 6. Rao, D., *Gas injection EOR-A new meaning in the new millennium*. Journal of Canadian Petroleum Technology, 2001. **40**(02).
 7. Dullien, F.A., *Porous media: fluid transport and pore structure*. Academic Press, Waterloo, Ontario, Canada, 2nd Edition, 1992, Chapter 2, 128-158.
 8. Lenormand, R., *Liquids in porous media*. Journal of Physics: Condensed Matter, 1990. **2**(S): p. SA79.
 9. Dullien, F.A., C. Zarcone, I.F. Macdonald, A. Collins, and R.D. Bochar, *The effects of surface roughness on the capillary pressure curves and the heights of capillary rise in glass bead packs*. Journal of Colloid and Interface Science, 1989. **127**(2): p. 362-372.
 10. Khorshidian, H., L. James, and S. Butt, *The Role of Film Flow and Wettability in Immiscible Gas Assisted Gravity Drainage*, presented in part at the International Symposium of the Society of Core Analysts Colorado, USA, August 2016.
 11. Piri, M. and M.J. Blunt, *Three-phase threshold capillary pressures in noncircular capillary tubes with different wettabilities including contact angle hysteresis*. Physical Review E, 2004. **70**(6): p. 061603.
 12. Helfferich, F.G., *Theory of multicomponent, multiphase displacement in porous media*. Society of Petroleum Engineers Journal, 1981. **21**(01): p. 51-62.
 13. Bahralolom, I.M. and F.M. Orr Jr, *Solubility and extraction in multiple-contact miscible displacements: comparison of N₂ and CO₂ flow visualization experiments*. SPE Reservoir Engineering, 1988. **3**(01): p. 213-219.
 14. Campbell, B.T. and F.M. Orr Jr, *Flow visualization for CO₂/crude-oil displacements*. Society of Petroleum Engineers Journal, 1985. **25**(05): p. 665-678.

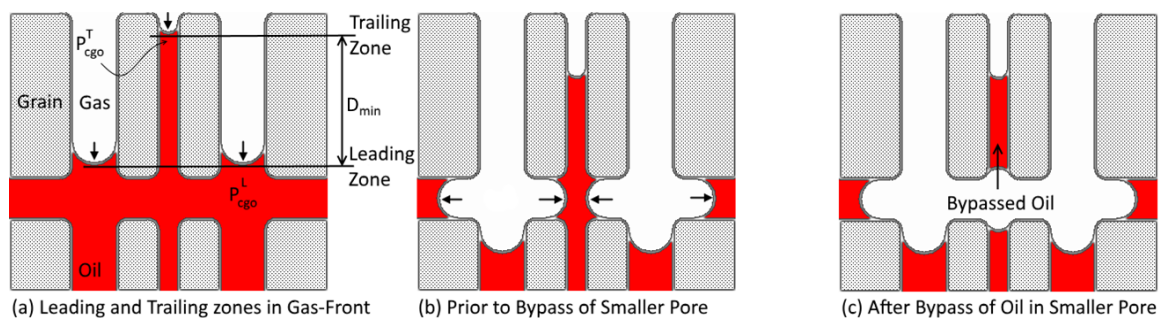


Fig. 1: Schematic representation of the bypass of oil with leading zones in the gas-front

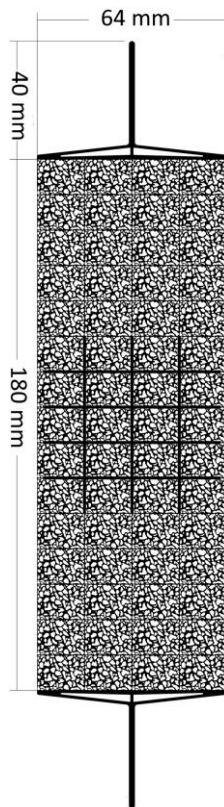


Fig. 2: Designed pore network of micromodel

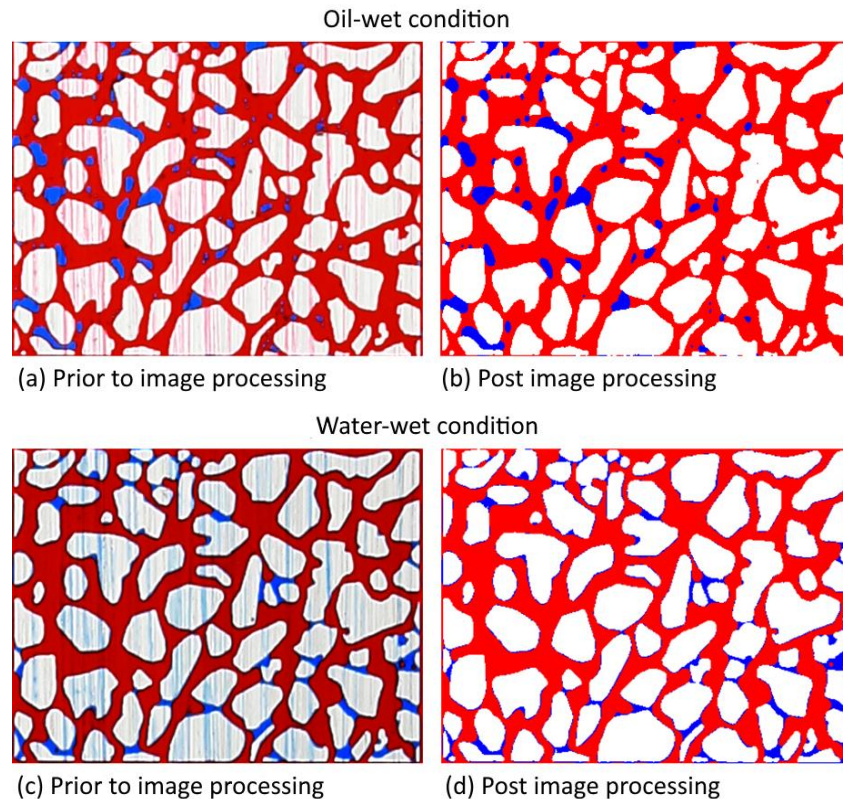


Fig. 3: The repeated pattern of micromodel prior and after image processing (red: oil - blue: water, pattern size: 16×12 mm)

Table 1: Interfacial tensions between fluids under experiment conditions

Bulk Fluid	Drop Fluid	Pressure (bar)	IFT (mN/m)
C ₃ H ₈	Water	4.0	63.4±1.2
C ₃ H ₈	Water	8.4	47.3±1.2
C ₃ H ₈	Oil	4.0	15.8±0.2
C ₃ H ₈	Oil	8.4	Miscible
CO ₂	Water	4.0	71.3±1.8
CO ₂	Oil	4.0	21.8±0.3
Varsol	Water	4.0	31.5±0.8

Table 2: Composition of Varsol™ oil

Component	Composition (wt%)
C8	1%
C9	8%
C10	27%
C11	38%
C12	25%
C13	2%
Sum	100%

Table 3: Summary of experimental results (uncertainty of calculated saturations: ±2%)

Wettability	Oil-wet				Water-wet				
	CO ₂		C ₃ H ₈		CO ₂		C ₃ H ₈		Miscible
Replication	1	2	1	2	1	2	1	2	1
Initial Oil Saturation (PV)	0.91	0.86	0.84	0.79	0.83	0.74	0.75	0.75	0.76
Initial Water Saturation (PV)	0.09	0.14	0.16	0.21	0.17	0.26	0.25	0.25	0.24
Oil Saturation at Breakthrough (PV)	0.30	0.31	NA	0.28	0.36	0.34	0.33	0.33	NA
Water Saturation at Breakthrough	0.09	0.14	NA	0.21	0.17	0.26	0.25	0.25	NA
Ultimate Oil Saturation (PV)	0.23	0.19	0.20	0.21	0.32	0.30	0.29	0.27	< 0.01
Ultimate Water Saturation (PV)	0.07	0.11	0.13	0.20	0.17	0.24	0.24	0.25	0.24
Ultimate Oil Recovery Factor (%)	76%	78%	84%	82%	61%	59%	74%	76%	> 99%

NA: Data Not Available * IOIP: Initial Oil in Place

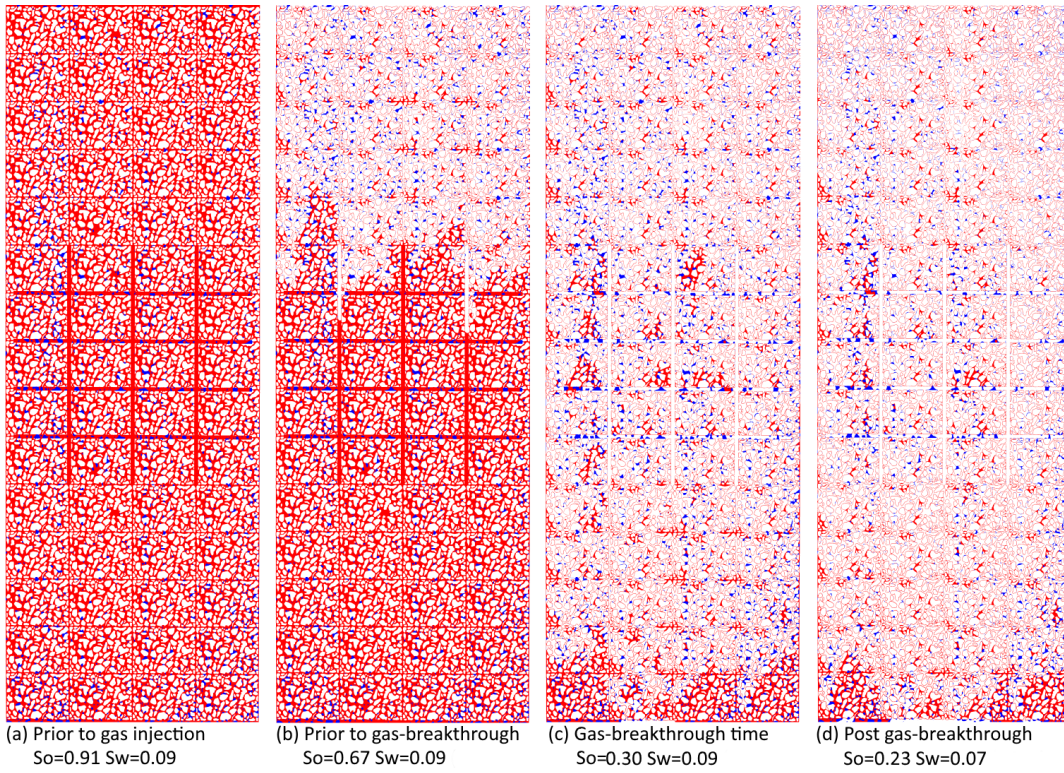


Fig. 4: Immiscible GAGD experiment performed with CO₂ in oil-wet conditions (processed image, red: oil – blue: water)

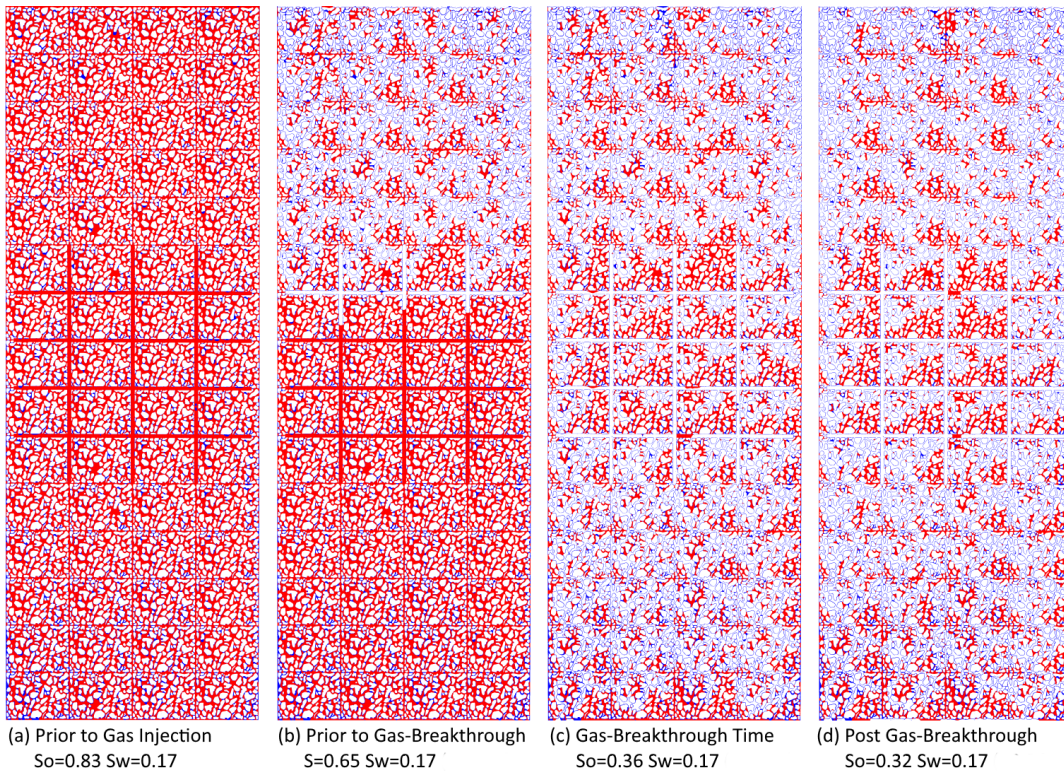
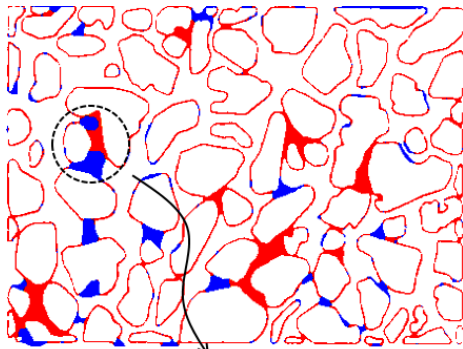
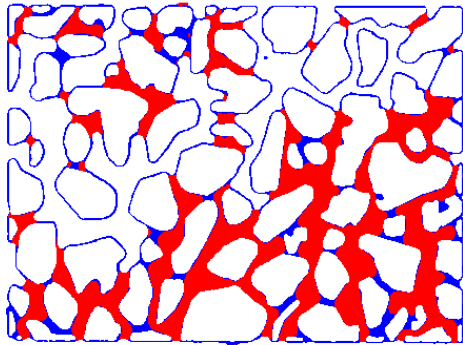


Fig. 5: Immiscible GAGD experiment performed with CO₂ in water-wet conditions (processed images, red: oil – blue: water)

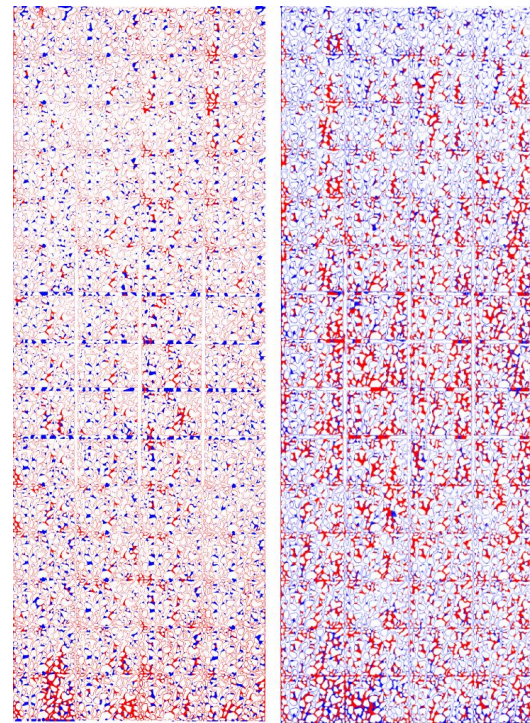


(a) Oil-wet (water-blocked pore)



(b) Water-wet

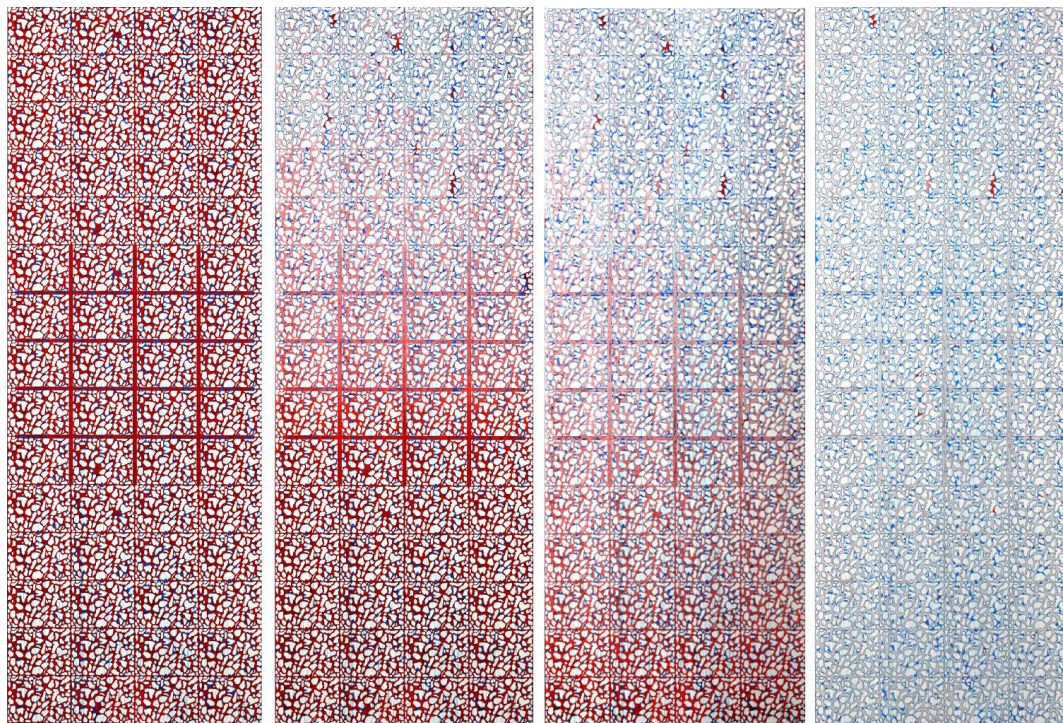
Fig. 6: Residual oil (red) and water (blue) in oil-wet and water-wet conditions (processed images)



(a) Oil-wet
So=0.20 Sw=0.13

(b) Water-wet
So=0.30 Sw=0.25

Fig. 7: Immiscible GAGD performed with C₃H₈ in oil-wet and water-wet conditions (processed images, red: oil, blue: water)



(a) Prior to gas injection
So=0.78 Sw=0.22

(b) Prior development of miscible contact

(c) Developed miscible contact after 0.85 PV production

(d) After 2.00 PV production
So < 0.01 Sw=0.21

Fig. 8: Miscible GAGD experiment performed with C₃H₈ in water-wet conditions (unprocessed images, red: oil – blue: water – pink: oil with dissolved gas)